Wireless Capsule Endoscope for Targeted Drug Delivery: Mechanics and Design Considerations

Stephen P. Woods, and Timothy G. Constandinou, *Senior Member, IEEE*

***Abstract*—This paper describes a platform to achieve targeted drug delivery in next generation wireless capsule endoscopy. The platform consists of two highly novel sub-systems: one is a micro-positioning mechanism which can deliver 1 ml of targeted medication and the other is a holding mechanism which gives the functionality of resisting peristalsis. The micro-positioning mechanism allows a needle to be positioned within a 22.5^o segment of a cylindrical capsule and be extendible by up to 1.5 mm outside the capsule body. The mechanism achieves both these functions using only a single micro-motor and occupying a total volume of just 200 mm^3. The holding mechanism can be deployed diametrically opposite the needle in 1.8 s and occupies a volume of just 270 mm^3. An in-depth analysis of the mechanics is presented and an overview of the requirements necessary to realise a total system integration is discussed. It is envisaged that the targeted drug delivery platform will empower a new breed of capsule micro-robots for therapy in addition to diagnostics for pathologies such as ulcerative colitis and small intestinal Crohn's disease.**

***Index Terms*—wireless capsule endoscopy, gastrointestinal (GI) tract, targeted therapy, micro-robot, pill robot.**

I. Introduction

THERE are a number of wireless capsule endoscopes (WCE) available for detecting and diagnosing pathologies of the gastrointestinal (GI) tract such as small intestinal Crohn's disease, obscure gastrointestinal bleeding (OGIB) and small intestinal tumours.

One such capsule is the M2A developed by Given Imaging Ltd. [1] in 2000. This system was developed specifically for examining the small intestines as conventional endoscopes cannot reach the total length of the GI tract [2]. Its small size of 11.0 mm in diameter $\times$ 25.0 mm long allows it to pass through the GI tract under natural peristalsis pressure. Another similar system is the EndoCapsule by Olympus [3]. These systems use onboard CMOS or CCD-based image sensors to take pictures of the intestinal wall. The pictures can be transmitted to a device worn by the patient for later evaluation. A detailed review of WCE is reported in [4].

Current WCE systems in general do not have the functionality or the onboard capacity to treat pathologies of the GI tract, such as ulcerative colitis, with medication as they are limited to diagnostic use. However there is a clinical need to target and treat these pathologies [5] hence endeavours have been made by researchers such as Philips Electronics with IntelliCap [6], Innovative Devices LLC with the InteliSite [7] and Phaeton Research with the Enterion capsule [8] to perform regional drug absorption services. These systems are capable of delivering up to 1 ml of medication to a region of the GI tract such as the jejunum, ileum, ascending colon or descending colon either through the progressive release of medication over a period of time or through a bolus form.

Manuscript received XXX, revised YYY, accepted ZZZ.

This work was in part supported by Duckworth and Kent Ltd.

The authors are with the Department of Electrical & Electronic Engineering and Centre for Bio-Inspired Technology, Institute of Biomedical Engineering, Imperial College London, South Kensington Campus, London SW7 2AZ, United Kingdom, email: {s.woods09,t.constandinou}@imperial.ac.uk

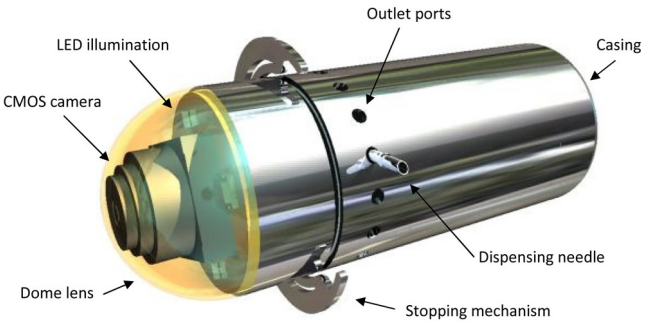

Fig. 1. Micro-robot concept design capable of resisting peristaltic pressure through an integrated holding mechanism and delivering 1 ml targeted medication. Holding mechanism shown partially open and the needle fully extended to 1.5 mm outside the capsule body

The delivery methods employed by these devices prevents the direct targeting of specific pathogens such as tumours or ulcers as the medication is spread over a section of lumen due to the constant movement from peristalsis, further they have no means of stopping and holding their position.

This paper presents a platform for delivering a targeted dose of medication in a confined compliant tubular environment. The platform comprises a holding mechanism and a needle positioning mechanism which are integrated into a WCE. This integration gives increased functionality allowing the WCE to be used for targeted drug delivery in the GI tract. Specifically this paper focuses on the two key mechanisms and is organised as follows: Section II introduces the concept and requirements, Section III describes the holding mechanism for resisting peristalsis, Section IV describes the targeting/delivery mechanism, Section V discusses additional platform considerations required to complete a system realisation, and Section VI concludes this work.

II. Concept and Design Requirements

Conventional WCE have sufficiently small geometry to allow them to pass through the small intestines and navigate the ileocolic valve without becoming an obstruction. However the clinical need to target a specific location or feature within the GI tract for medication delivery or examination of the

intestinal wall would require the WCE to stop. Fig. 1 shows a micro-robot concept design capable of resisting peristaltic pressure through the deployment of an integrated holding mechanism and targeted drug delivery through the activation of a needle. The needle has the ability to be positioned in a 360 degree envelope. Simultaneously the holding mechanism can stay diametrically opposite the needle guaranteeing penetration of the GI tract wall.

A. Movement Analysis of the GI Tract

Once swallowed the WCE will pass through the elementary canal. The particular section of interest for diagnosis and treatment is the small intestines as this section is very difficult to access. The small intestines comprise of the duodenum, the jejunum and the ileum. These three sections make up the longest part of the alimentary canal at 6.25 m [9]. The duodenum is C shaped and its mouth, the ileocolic valve, extends from the stomach giving this section a degree of stability. The jejunum and the ileum are free to move however their natural state is collapsed.

In order to process foodstuff, a liquid mixture called chyme, the small intestines uses a series of movement patterns. These patterns, segmentation and peristalsis [10], cause the chyme to progress through the tract. Segmentation is a contraction of the duodenum for the purpose of mixing food. There are two processes involved, they are eccentric contractions and concentric contraction. The first generates very little intraluminal pressure and the second can generate pressures as high as 20 mmHg [10]. The frequency of the contractions is dependent on eating patterns, becoming stronger as chyme is being processed. Peristalsis is the process of moving chyme through the intestinal tract from the stomach to the colon by means of a series of muscle contractions acting in a wave pattern. The muscle contraction acts in two planes, circumferential and longitudinal. Miftahof (2005) [11] has developed a mathematical model to describe the dynamics of the electromechanical wave phenomenon of a segment of the gut. They report that the active force of contraction in the longitudinal direction to have an amplitude of 26.9 g/cm and an amplitude of 17.2 g/cm in the circumferential direction. For a conventional WCE with dimensions of 11.0 mm diameter $\times$ 25.0 mm long, the circumferential and longitudinal amplitudes translate into 421.8 mN and 911.9 mN respectively. These estimated forces have been used as a guide in the design analysis of the holding mechanism.

B. Resisting Peristalsis and Geometrical Constraints

There are three methods employed for halting the progress of a WCE by enabling it to resist the natural movement from peristalsis. One utilises micro-actuator mechanisms embedded within the capsule, such as the paddling based microrobot developed by Park et al. (2007) [12]. The second approach exploits external magnetic fields to control the position of the capsule and the third approach applies a stimulus to GI tract to inhibit peristalsis [13].

There has been much development in the field of magnetic control of WCE such as the magnetic shell employed by Carpi et al. [14]. This system looks to modify existing WCE with the addition of a magnetic shell. The shell can be used to guide the WCE by means of an external magnetic field, however this system requires large equipment to perform the procedure and there is also an increase in the diameter of the WCE.

To overcome peristalsis a holding mechanism compact enough to fit within the micro-robot yet leave sufficient space for medication and other features is required. There have been a number of systems employed by researchers to stop the micro-robot, such as insufflation of the tract using balloons or expanding legs [15]. However these systems exhibit limitations. In the case of the expanding legs they are driven by a leadscrew which is powered by a micro-motor. The leadscrew and the micro-motor are axially aligned with the micro-robot. This configuration requires a substantial amount of space and presents problems of force translation through the legs due to the lever effect.

C. Target Technical Specifications

The overall geometry of the micro-robotic system will be greatly influenced by the limitations imposed by swallowing and on its ability to navigate natural obstacles such as the ileocolic valve without becoming an obstruction. A patient's ability to swallow a required volume will vary from person to person, therefore a standard volume must be chosen which will be suitable for the majority of patients. Research carried out by Connor et al. (2009) shows that a volume of 3.0 cm^3 can be swallowed [16]. This maximum target volume will be required to house all the components necessary to perform targeted therapy and micro-scale diagnosis. Table I lists the overall technical requirements for the micro-robot platform.

TABLE I
OVERALL TECHNICAL REQUIREMENTS

Requirement	Specification
Micro-robot volume	maximum 3.0 cm^3
Sensing	pH, temp and pressure
Vision	CMOS and optical dome
Illumination	4 white LEDs
Power source	onboard battery
Tracking	RF and time
Telemetry	bidirectional
Attaining equilibrium	holding
Delivering therapy	liquid medication
Drug reservoir	1 ml

D. System Operation Overview

The main sequence of events required to perform a procedure to deliver targeted therapy to the GI tract can be seen in Fig 2. The procedure starts with the patient ingesting the WCE. Once the capsule passes through the stomach and enters the small intestines it can begin to transmit images to the operator via an RF link. The real-time images and sensor data will be displayed on an external PC. The operator will use the data to identify an already defined target site. Once the target site has been reached the operator will remotely

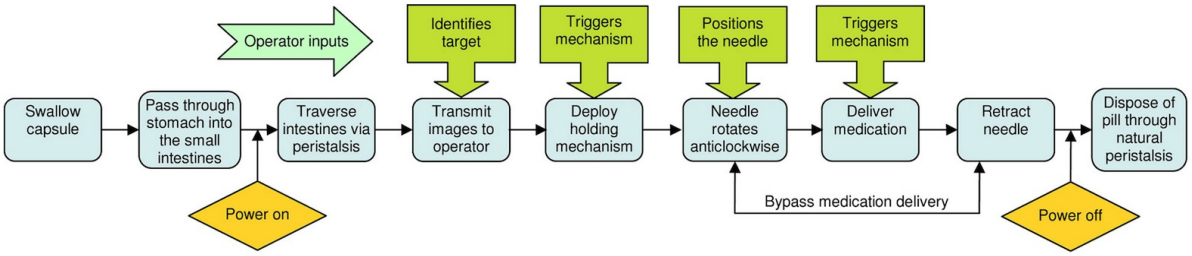

Fig. 2. Flow diagram showing the key stages of operation for a procedure to deliver targeted therapy to the GI tract using a remotely operated WCE

deploy the holding mechanism. The operator can now rotate the needle into any one of 16 predefined positions, the position will be based on observational data received just before the deployment of the holding mechanism. The needle can now be advanced into the GI tract wall and the medication released. The targeting mechanism is designed such that it gives the operator the ability to reposition the needle before the medication is delivered. Finally the capsule will be dispelled through natural peristalsis movement.

III. Holding Mechanism

The holding mechanism (Fig. 3a) uses a single micro-motor to open and close two legs. The two legs are connected to a central support via two pinned leg ties. The two-legged design utilises a micro-motor which is orientated in a vertical position (Fig. 4a). The micro-motor is connected to a bevel gear set, this allows the micro-motor's rotation to be translated through 90 degrees. The bevel gear drives a gear train of spur gears which drive the legs in and out (Fig. 3b & 4b). This novel configuration reduces the micro-motor's RPM. The reduction in RPM will result in a multiplication of the micro-motor's torque, this will give the legs the strength required to distend the GI tract wall and hold the micro-robot in place.

To secure the micro-robot in place the holding mechanism will be required to expand to a size which is sufficiently large that it resists the natural movement from peristalsis. This is achieved through an increase in circumference of the micro-robot. The holding mechanism begins with a circumference of 34.5 mm, however when activated the mechanism increases in size to produce a circumference of 60.4 mm, which is an increase of 75%. This can be further increased to 71.25 mm by simply modifying the profile of the legs to increase the surface area in contact with the GI tract wall.

The method by which the legs open and close poses the potential risk of tissue becoming trapped in the mechanism, however the orientation of the legs combined with their smooth rounded ends will act to prevent the naturally collapsed GI tract wall from penetrating the capsule's leg cavity.

The advantage of the vertical configuration of the micro-motor is that it allows for a very compact design ($270\,mm^3$) resulting in the most efficient use of space. The two legs, central support, leg ties and the micro-robot case will absorb the load from the GI tract wall. The compact gearing allows the rate at which the legs are deployed to be controlled by the ratio of the gear train.

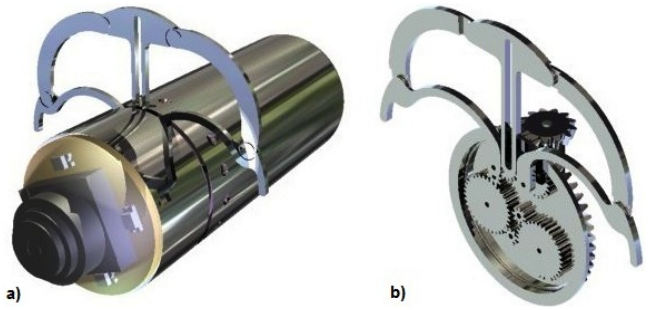

Fig. 3. Holding mechanism concept which utilises a vertically orientated micro-motor to give the WCE the ability to overcome peristalsis a) and a 3D internal view of the gear train b)

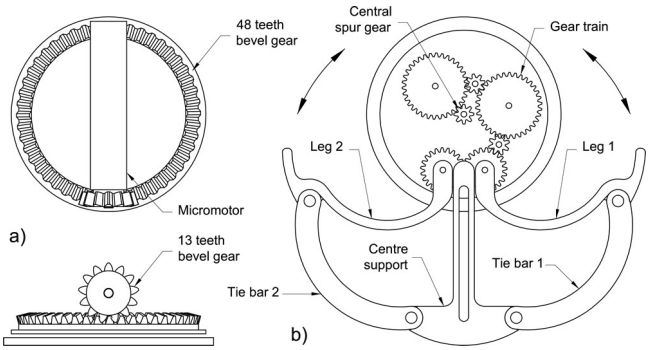

Fig. 4. Holding mechanism design showing: a) 13 teeth and 48 teeth bevel gears set, b) gear train and legs in the fully extended position. The central spur gear is driven by the 48 teeth bevel gear.

A. Gear Train

For the holding mechanism to operate at a safe speed the micro-motor will require the gear train to slow it down. The chosen micro-motor is manufactured by Faulhaber and already has an integral gearbox which reduces the 20,000 RPM by a factor of 13:1. This results in a starting RPM of 1,538 RPM, which is significantly high, therefore further reductions will be achieved from the gear train. The output speed of a gear train can be estimated from the following equation:

$$RPM_{out} = \frac{N_{d1} \times N_{d2} \times N_{d3} \times N_{d4} \times RPM_{in}}{N_{f1} \times N_{f2} \times N_{f3} \times N_{f4}} \quad (1)$$

Where RPM_{in} is the input speed, N_{d1} is the number of teeth on the driving gear and N_{f1} is the number of teeth on the follower gear. This formula can be applied to the gear train with a selection of gear teeth to determine the output RPM,

Table II.

TABLE II
ESTIMATED GEAR TRAIN OUTPUT FROM AN INPUT OF 1,538 RPM

Gear stages	Micromotor and bevel gear	Bevel gear and spur gear	Second stage spur gear	Output spur gear
No. of teeth on driver (d)	13	8	8	8
No. of teeth on follower (f)	48	34	34	22
Output RPM	417.93	98.34	23.14	8.41

As can be seen from Table II the number of teeth on the follower gears is higher than the number of teeth on the driving gears, this is to ensure a rapid reduction in RPM in the minimum amount of space. The target is to deploy the holding mechanism as slowly as possible as this will reduce the potential for trauma to the GI tract wall from the legs and supports. However there are limitations to the number of teeth which can be used as the chosen gear module, which is the ratio of the pitch diameter to the number of teeth on the gear, determines the overall geometry of the gear. The chosen bevel gear module is 0.2 this results in a maximum number of teeth of 48 and an overall gear diameter of 10.0 mm (Fig. 4a) as the gear has the overall limiting factor of the diameter of the micro-robot. The spur gears use a module of 0.1 this results in a maximum number of teeth of 34 as the gears are required to be linked together in a train (Fig. 4b) they are therefore limited again to the overall diameter of the micro-robot.

The gear train results in a reduction of 1,538 RPM to 8.4 RPM. This reduced output speed will deploy the legs in approximately 1.8 seconds, altering the number of teeth on the driver or follower will increase or decrease this figure.

An important function of the gear train is to transmit power from the micro-motor to the legs, this will enable the legs to distend the luminal wall and hold the micro-robot in position. The power transmitting capacity of a gear train can be determined by the following formula:

$$T_{out} = \frac{N_{f1} \times N_{f2} \times N_{f3} \times N_{f4} \times T_{in}}{N_{d1} \times N_{d2} \times N_{d3} \times N_{d4}} \tag{2}$$

Where T_{in} is the input torque, N_{f1} is the number of teeth on the follower gear and N_{d1} is the number of teeth on the driving gear. Applying this formula to the gear train and using 0.15 mNm torque generated by the Faulhaber micro-motor as the input torque (T_{in}) results in an estimated output torque (T_{out}) of 27.5 mNm.

B. Analysis of Holding Mechanism Arms

To attain a state of equilibrium the external forces acting on the micro-robot must be balanced for any given orientation, however angles less than 90 degrees from the horizontal can be neglected from the equilibrium analysis, as in the worst case the load would be acting vertical to the horizontal resulting in a multiplication factor of $\sin 90$ which equals 1 hence producing no net increase in load. Fig. 5 shows the external forces acting on the legs of the micro-robot. For the force analysis the contact area has been divided into 6 contact points as these points will be in continuous contact with the GI tract wall throughout the deployment of the mechanism.

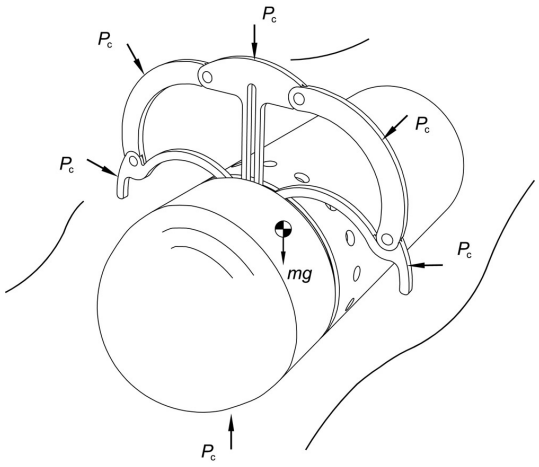

Fig. 5. External radial peristaltic force (P_c) acting on the micro-robot at 6 positions

As can be seen from Fig. 5 the external forces acting on the micro-robot's legs are the circumferential peristaltic force (P_c), the linear peristaltic forces are neglected as they do not contribute to the holding function and through FEA analysis it has been shown that they are not sufficiently strong to cause any deformation of the mechanism. Using the figures determined by Miftahof (2005) [11] the circumferential amplitude of 26.9 g/cm results in an estimated load of 720.8 mN for the total circumferential contact area of the extended legs and micro-robot's body.

The micromotor employed to drive the legs must be capable of delivering an equivalent force to the legs to maintain a state of equilibrium. The force acting at each point of contact (P_c) can be estimated by the following formula:

$$P_c = \frac{F_c + mg}{6} \tag{3}$$

Where F_c is the circumferential force from the GI tract wall and mg is the weight of the micro-robot.

The load acting at each point equates to 120.1 mN, however this load will work towards preventing the legs from opening.

C. Load Points (P_c) Contributing to Torque

The process of operating the legs from the stored position to the fully extended position results in the circumferential force from the GI tract wall (P_c) acting towards the centre of the micro-robot. However only the perpendicular component force (F_{p1}) will be working to prevent the legs from opening. This is illustrated for leg 1 in Fig. 6.

The perpendicular component force F_{p1} (Fig. 6) can be estimated for a leg movement through zero degrees to 90 degrees using the following formula:

$$F_{p1} = P_c \left(\frac{c(\sin A)}{\sqrt{b^2 + c^2 - 2bc(\cos A)}} \right) \tag{4}$$

The perpendicular component force F_{p2} acting on tie bar 1 can be seen in Fig. 7 and can be estimated as follows:

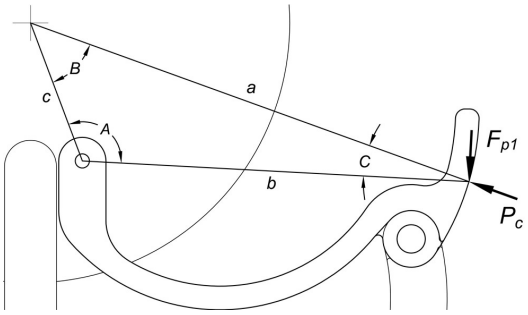

Fig. 6. Component force (F_{p1}) of the radial peristaltic force (P_c) acting on the micro-robot's leg

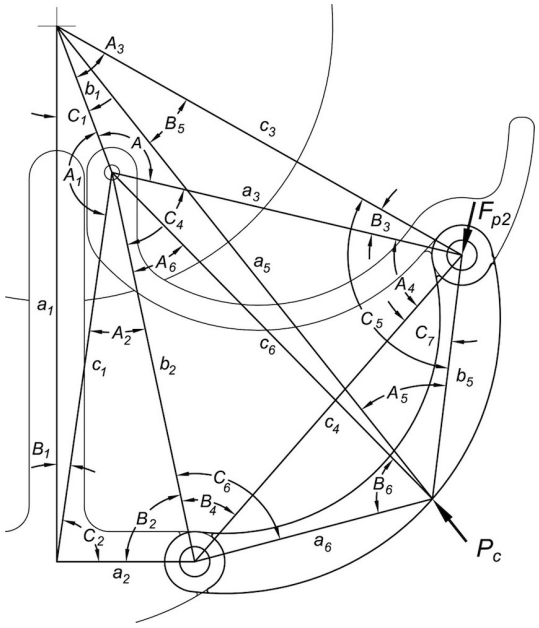

Fig. 7. Component force (F_{p2}) of the radial peristaltic force (P_c) acting on the micro-robot's tie bar. The tie bar links the leg to the centre support

$$F_{p2} = P_c \cos\left[\tan^{-1}\left(c_3\left(\frac{\sin C_5}{b_5 - (c_3 \cos C_5)}\right)\right)\right] \sin\left[\cos^{-1}\left(\left({a_3}^2 + {b_2}^2 + {c_4}^2\right) - \left(\frac{{b_2}^2}{2a_3c_4}\right)\right) + C_7\right] \quad (5)$$

The radial peristaltic force (P_c) acting on the centre support (Fig. 8) would be split between the two pivot points linking the two tie bars, however the sum of the two points would count towards the torque requirement. As the geometry and loading are symmetrical only one side of the centre support requires analysis, this can be seen in Fig. 8 and can be estimated as follows:

$$F_{p3} = \left[\frac{P_c}{\sin(180 - (C_3 + B_2 + C_1))}\right] \sin\left[\tan^{-1}\left(\frac{a_2 \sin A_3}{b_3 - (b_2 \cos A_3)}\right)\right] \quad (6)$$

Equation 6 uses the total peristaltic force (P_c) therefore the resulting component force F_{p3} represents the total component force from both pivot points of the centre support.

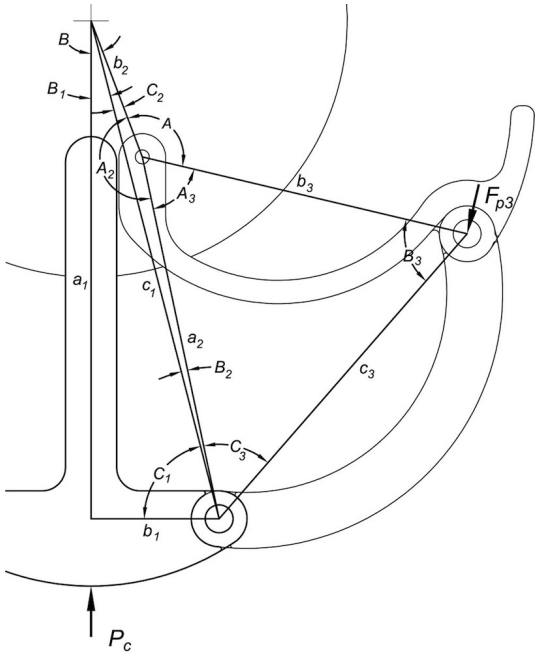

Fig. 8. Component force (F_{p3}) of the radial peristaltic force (P_c) acting on the micro-robot's centre support

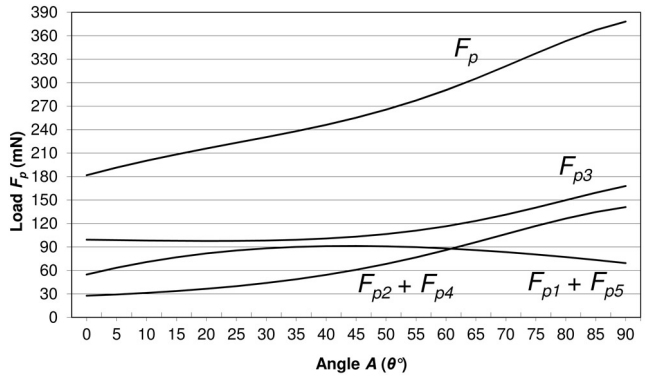

Fig. 9. Graph showing the individual perpendicular component forces $F_{p1}, F_{p2}, F_{p3}, F_{p4}$ and F_{p5} generated by the GI tract acting on the holding mechanism and the total combined load F_p which will act to prevent the holding mechanism from operating

The three individual perpendicular component forces F_{p1}, F_{p2} and F_{p3} can be combined with F_{p4} the perpendicular component forces for tie bar 2 and F_{p5} the perpendicular component forces acting on leg 2 to find the maximum load which will be delivered to the micro-motor through the zero to 90 degree leg movement. Fig. 9 shows a plot of the individual loads through the full movement and the resulting combined load (F_p).

The result of the combined plots (Fig. 9) shows the maximum load of 378.15 mN acting on the final gear in the gear train to be at 90 degrees, this results in a torque of 2.78 mNm acting on the gear. However the estimated results of equation 2 show an output torque (T_{out}) for the gear train to be 27.5 mNm this gives a high margin of safety before the micro-motor stalls. The holding mechanism has been designed to withstand the estimated force the GI tract wall can generate. A

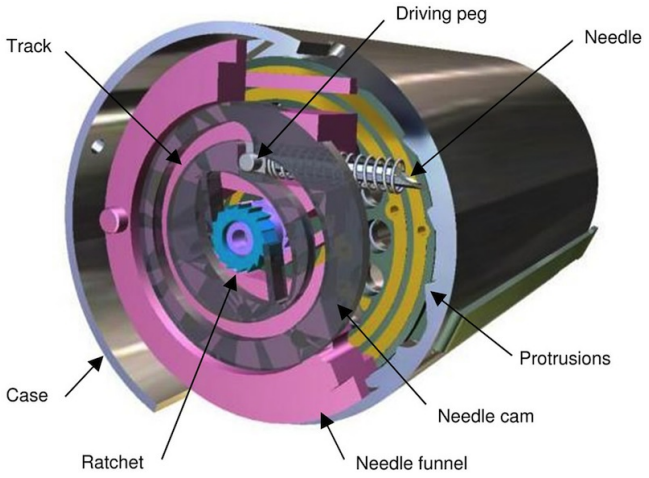

Fig. 10. Needle positioning mechanism assembly with material removed for clarity. Needle shown in the fully retracted position

system validation including *in-vivo* measurements are required to verify these results.

The 6 point loads have been used to confirm the stability of the mechanism through FEA analysis. Using the FEA process the thickness of the arms was optimised however the areas that contact the GI tract wall may be increased in future trials to limit any potential trauma to the GI tract wall.

IV. Targeting and Drug Delivery Mechanism

A. Needle Positioning Mechanism

A single micro-motor orientated along the axis of the micro-robot's body is used to drive the needle positioning mechanism (Fig. 10). The needle positioning mechanism utilises a 1.5 mm diameter $\times$ 10.5 mm long micro-motor manufactured by Namiki, a needle funnel, a movable needle, a needle cam and two opposing ratchets. Also features integral to the micro-robot's body are required (protrusions). The sequence of operation is to firstly position the needle angularly followed by the extension of the needle and delivery of the medication, then the needle is retracted. The supply of medication will be stored in a sealed section of the body and be delivered through the needle by means of a piston. Rapid delivery of the medication will be achieved through the activation of a conical shape memory alloy (SMA) compression spring. Activating the spring by means of the Joules effect will remove the need for a bulky complex trigger system to release the spring.

The needle positioning mechanism is capable of positioning the needle at a number of points in a 360 degree envelope, however for the purpose of prototyping 16 fixed positions equally spaced have been chosen. The angular positioning of the needle is achieved by the anticlockwise rotation of the micro-motor while the advancement and retraction of the needle is achieved by the clockwise rotation of the micro-motor.

B. Positioning the Needle

Manoeuvring the needle to a selected position is achieved by applying a negative voltage to the micro-motor. The negative voltage will cause the micro-motor to rotate in an anticlockwise direction. The needle funnel (Fig. 11a) rotates anticlockwise by virtue of a ratchet which is mounted on the micro-motor's driveshaft. The ratchet engages with a set of sprung legs which are integral to the needle funnel (Fig. 11b). The needle is engaged with the needle funnel and is carried round with it.

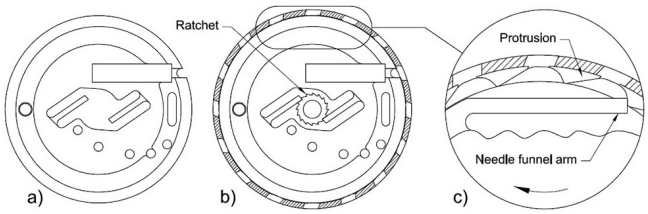

Fig. 11. Needle positioning mechanism: needle funnel a), ratchet driving the needle funnel, which has material removed b) and the needle funnel arm engaged with a protrusion c)

When the needle funnel is rotating anticlockwise an arm which protrudes from the side of the needle funnel rides over the top of a plurality of protrusions (Fig. 11c) on the inside face of the body. The function of these protrusions is to prevent the needle funnel from rotating clockwise when the motor is reversed. It achieves this by engaging the end of the arms with a parallel surface of the protrusion (Fig. 11c) preventing any further movement clockwise and aligning the needle with one of the 16 fixed ports on the micro-robot's body.

C. Operating the Needle

Applying a positive voltage to the micro-motor reverses its direction, this disengages the needle funnel ratchet from its sprung legs and engages the needle cam ratchet with a set of sprung legs that are integral to the needle cam (Fig. 12).

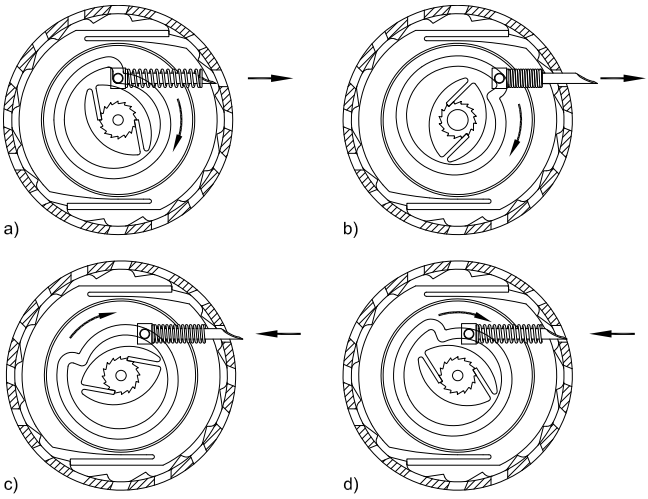

Fig. 12. 360 degree needle cam operating cycle: stored position a), full stroke b), needle returning to the stored position c), and retracted position d)

When engaged the ratchet drives the needle cam in a clockwise direction. The needle is engaged with a track in the needle cam by means of a driving peg mounted on the side of the needle (Fig. 12). The track is shaped to convert

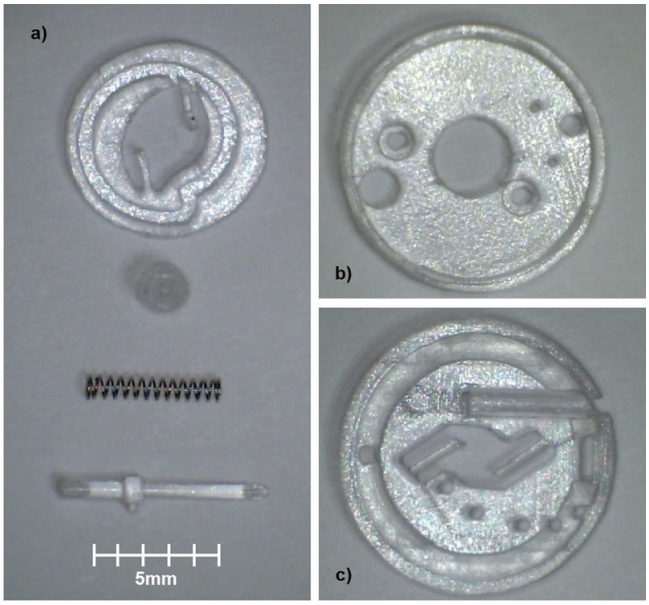

Fig. 13. 1:1 scale SLA prototypes. a) shows the needle cam, ratchet, spring and needle combined with the driving peg b) shows the retaining cover and c) is the needle funnel

the rotational motion of the cam into a variable linear motion. This linear motion allows the advancement and retraction of the needle.

Fig. 12 shows the sequence of operation for the extension and retraction of the needle. Fig. 12a shows the needle in the stored position, this is the position the needle will be in when the micro-robot is swallowed and travels through the GI tract to the target site. A compression spring is used to ensure the driving peg maintains contact with the track and also that the needle returns to the start position. Fig. 12b shows the needle at full extension giving a reach of approximately 6.9 mm radius and a stroke length of 2.0 mm. The design of the cam utilises a direct linear movement so that a positive force can be delivered to the needle which will be required to penetrate the wall of the GI tract. Fig. 12c shows the needle retracting by virtue of the track slowly spiralling inwards and the pressure exerted by the spring. Fig. 12d shows the needle returning to the stored position once the medication has been delivered. Further design analysis of the targeting mechanism has been described in detail in previous work [17].

Fig. 13 shows the component parts of the needle positioning mechanism. All the parts except the stainless steel spring have been prototyped using a high resolution stereolithography (SLA) manufacturing process. The one-to-one scaled prototypes are manufactured from Accura 60 which is a resin with similar mechanical properties to polycarbonate.

The assembled needle positioning components can be seen in Fig. 14. Fig. 14a shows the needle funnel fitted with the needle and spring. Fig. 14b shows the needle cam mounted in the needle funnel and engaged with the needle's drive peg. Fig. 14c shows the ratchet mounted on a drive spindle and the cavity in the case which will house the targeting mechanism. Fig 14d shows the case fitted with the mechanism and the drive spindle at the rear.

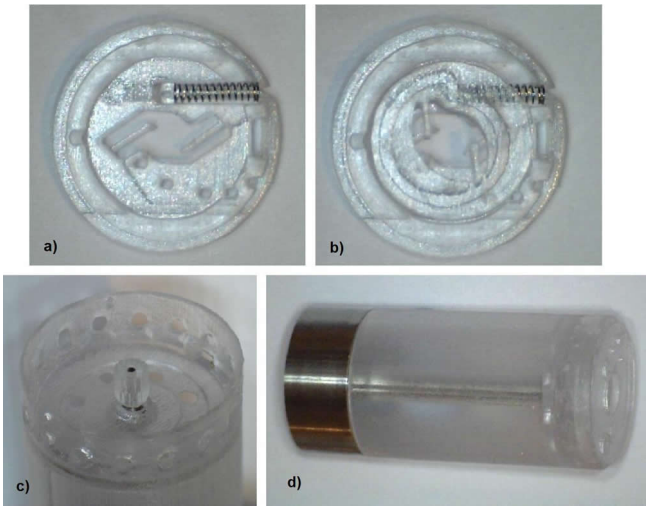

Fig. 14. Assembled needle positioning mechanism. a) shows the needle funnel, spring and needle assembled b) shows the needle cam in position c) shows the ratchet and case cavity and d) shows the case fitted with the mechanism and coupled to a drive spindle

The proof of concept prototypes perform within the allowable design limits with all the arms flexing and returning to their original positions. The spring allows the needle to advance 2.0 mm and then return back to rest.

V. Additional Platform Considerations

In order to complete a system realisation of a targeted drug delivery platform there are several aspects which, although outside the scope of this paper, are necessary to realise. This section will detail these considerations:

A. Localisation

It is an important requirement that the location of the micro-robot is known when it passes through the GI tract [18]. The spatial information will be used to determine where potential pathologies have been located and hence give the ability to return to these sites for follow-up treatment.

One method reported in the literature for following the progress of a WCE through the GI tract is through the monitoring of the magnetic field strength of an on-board permanent magnet [19]. Using a magnetic tracking algorithm and a magnetoresistive sensor array attached to the skin the position and orientation of the micro-robot can be estimated. Figures reported by Wang et. al. (2006) [20] show average position errors of 3.3 mm and average orientation errors of 3 degrees, however the number of external sensors will determine the overall accuracy of the system.

A widely used approach to localisation is through the monitoring of electromagnetic waves [19]. Radio frequency triangulation is employed on the M2A by Given Imaging. This method utilises the received signal strength of the images which are being transmitted to eight external receivers to determine the position of the device. The average position error of this method is 37.7 mm however this method is limited to 2D positioning [21].

There are alternative methods to localisation such as gamma scintigraphy. This method is employed on the InteliSite [7] by Innovative Devices LLC. The capsule can be tracked through the GI tract using gamma scintigraphy which will detect Indium (111In) or Technetium (99mTc) gamma isotopes that have been incorporated into the capsule. However the locational accuracy of the system is limited as capsule orientation cannot be determined and only the capsule's general position within the GI tract can be ascertained.

It is intended that additional monitoring methods such as recording pH levels and transit time will be combined with a localisation method to give an overall indication of the capsule's location.

B. Electronics

It is crucially important to consider the various components and wiring in such a space-constrained design. Key electronic components include:

1) CMOS image sensor: This design uses a commercially-available subminiature image sensor manufactured by Toshiba (TCM8230MDA) with four white SMT LEDs manufactured by Agilent (HSMW-C191) integrated on a PCB.

2) Rotary encoder and wiring: The micro-robot can be split into four sections: the visualisation and processing section, the needle positioning mechanism, the holding mechanism and the power supply section. Fig. 15 highlights these sections with a cut-through view of the micro-robot.

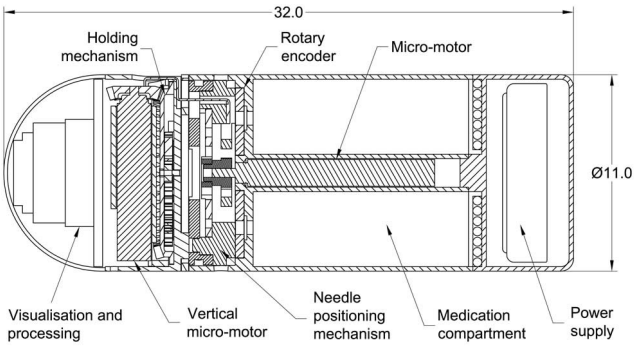

Fig. 15. Cut-through view of the micro-robot with the four main sections labeled

The configuration of the four sections of the micro-robot presents problems of power delivery, specifically delivering power to the holding mechanism and the visualisation and processing section. This is due to the requirement that the holding mechanism can be deployed diametrically opposite the needle, as this requires the front section of the micro-robot to be able to rotate 360 degrees.

The solution is to run power lines on the outside of the body from the power supply to a rotary encoder board, this bypasses the need to disrupt the medication compartment. The rotary encoder board has four concentric tracks equally spaced. Contact pins held in the needle positioning mechanism can contact the tracks yet still remain free to rotate. A fifth contact pin is used in conjunction with a registration contact on the rotary encoder board to determine the angular position of the needle and holding mechanism.

3) Controller ASIC: The power management (i.e. DC/DC conversion), telemetry, timing and control are being implemented in a full-custom ASIC in a commercially-available 0.18 μm CMOS technology. Much of the specific circuit implementations will be based on previously reported systems [22]–[24].

C. Energy Requirements

As the space available for the power supply onboard the WCE is limited it is essential that the needle positioning mechanism and the holding mechanism can both operate with low power consumption. The energy requirements for both mechanisms have been estimated from the peak current consumption of the Namiki motor controller (SSD04) and the Faulhaber motor controller (BLD05002S) which are stated as 800 mA at 6 V and 400 mA at 7.5 V respectively. Three revolutions of the Namiki micro-motor are required for positioning and deployment of the needle; this is achieved in 3.8 s while the holding mechanism can complete a full opening and closing cycle in 1.78 s. Using a Lithium coin battery with a volume of 188 mm^3 and an energy density of 435 Wh/L (CR1025 Energizer) the mechanisms will consume at most 28.94 J of energy for each complete cycle which is only 9.8% of the available energy, offering the potential for multiple operations.

VI. Conclusion

In this paper the authors have presented a novel targeted drug delivery platform towards the realisation of a practical micro-positioning system and holding mechanism for targeted drug delivery in the small intestines. The platform can be used for the detection and treatment of pathologies of the GI tract such as Crohn's disease, small intestinal tumours such as lymphoma and small intestinal cancer.

It has been shown that the proposed needle positioning mechanism and the holding mechanism achieve the required functionality whilst occupying a combined volume of less than 470 mm^3. This is based on the proposed needle positioning mechanism and holding mechanism consuming a maximum of 28.94 J of energy per operation.

The targeted drug delivery platform has the control necessary to target a particular pathogen within the GI tract. It is envisaged that a delivery mechanism capable of delivering 1 ml of medication to the target site can be incorporated into the standard geometry of the WCE, with the combined needle positioning system, holding mechanism and delivery mechanism (including 1 ml of medication) occupying 60% of the total available volume.

The research so far has been focused on the analysis of the novel micro-positioning mechanism and the holding mechanism. During *in-vitro* testing and validation these systems will be tested to determine if the needle positioning mechanism has sufficient power to penetrate the GI tract wall and that the holding mechanism has sufficient power to overcome peristalsis. An area for consideration is the miniaturisation of the electronics and the development of a control system with a user interface.

ACKNOWLEDGMENT

The authors would like to thank Consultant Physician Nick Oliver for clinical insight and much useful discussion and Peter Pendergast, Head of Prototyping and Production at IDC Models Ltd. for his invaluable help in producing the prototypes.

REFERENCES

[1] G. D. Meron, "The development of the swallowable video capsule (M2A)," *Gastrointestinal Endoscopy*, vol. 52, pp. 817–819, 2000.

[2] P. Swain and A. Fritscher-Ravens, "Role of video endoscopy in managing small bowel disease," *Gut*, vol. 53, no. 12, pp. 1866–1875, 2004.

[3] D. R. Cave, D. E. Fleischer, J. A. Leighton, D. O. Faigel, R. I. Heigh, V. K. Sharma, C. J. Gostout, E. Rajan, K. Mergener, A. Foley, M. Lee, and K. Bhattacharya, "A multicenter randomized comparison of the endocapsule and the pillcam sb," *Gastrointestinal Endoscopy*, pp. 487–494, 2008.

[4] J. L. Toennies, G. Tortora, M. Simi, P. Valdastri, and R. J. Webster III, "Swallowable medical devices for diagnosis and surgery: the state of the art," *Journal of Mechanical Engineering Science*, vol. 224, pp. 1397–1414, 2010.

[5] N. I. Goldfarb, L. T. Pizzi, J. P. Fuhr, C. Salvador, V. Sikirica, A. Kornbluth, and B. Lewis, "Diagnosing crohn's disease: An economic analysis comparing wireless capsule endoscopy with traditional diagnostic procedures," *Disease Management*, vol. 7, pp. 292–304, 2004.

[6] A. Forgione, "In vivo microrobots for natural orifice transluminal surgery. current status and future perspectives," *Surgical Oncology*, vol. 18, pp. 121–129, 2009.

[7] I. Wilding, P. Hirst, and A. Connor, "Development of a new engineering-based capsule for human drug absorption studies," *Pharmaceutical Science & Technology Today*, vol. 3, pp. 385–392, 2000.

[8] P. J. Houzego, P. N. Morgan, P. H. Hirst, D. J. Westland, and I. R. Wilding, "Ingestible device for the release of substances at distinct locations in the alimentary canal," U.S. Patent US 006 884 239 B2, 2005.

[9] H. Gray, *Gray's anatomy*. Greenwich Editions, 2005.

[10] W. Xiaona, M. Q. H. Meng, and C. Yawen, "Physiological factors of the small intestine in design of active capsule endoscopy," *Annual International Conference of the IEEE Engineering in Medicine and Biology Society (EMBS)*, pp. 2942–2945, 2005.

[11] R. N. Miftahof, "The wave phenomena in smooth muscle syncytia," *In Silico Biology*, vol. 5, pp. 479–498, 2005.

[12] H. Park, S. Park, E. Yoon, B. Kim, J. Park, and S. Park, "Paddling based microrobot for capsule endoscopes," in *IEEE International Conference on Robotics and Automation*, 2007, pp. 3377–3382.

[13] S. H. Woo, T. W. Kim, and J. H. Cho, "Stopping mechanism for capsule endoscope using electrical stimulus," *Medical & Biological Engineering & Computing*, vol. 48, pp. 97–102, 2010.

[14] F. Carpi, S. Galbiati, and A. Carpi, "Controlled navigation of endoscopic capsules: concept and preliminary experimental investigations," *IEEE Transactions on Biomedical Engineering (TBE)*, vol. 54, pp. 2028–2036, 2007.

[15] P. Valdastri, R. J. Webster, C. Quaglia, M. Quirini, A. Menciassi, and P. Dario, "A new mechanism for mesoscale legged locomotion in compliant tubular environments," *IEEE Transactions on Robotics*, vol. 25, pp. 1047–1057, 2009.

[16] A. Connor, P. Evans, J. Doto, C. Ellis, and D. E. Martin, "An oral human drug absorption study to assess the impact of site of delivery on the bioavailability of bevirimat," *Journal of Clinical Pharmacology*, vol. 49, pp. 606–612, 2009.

[17] S. P. Woods and T. G. Constandinou, "Towards a micropositioning system for targeted drug delivery in wireless capsule endoscopy," *Annual International Conference of the IEEE Engineering in Medicine and Biology Society (EMBS)*, pp. 7372–7375, 2011.

[18] G. Ciuti, A. Menciassi, and P. Dario, "Capsule endoscopy: From current achievements to open challenges," *IEEE Reviews in Biomedical Engineering*, vol. 4, pp. 59 –72, 2011.

[19] T. D. Than, G. Alici, H. Zhou, and W. Li, "A review of localization systems for robotic endoscopic capsules," *IEEE Transactions on Biomedical Engineering (TBE)*, vol. 59, no. 9, pp. 2387–2399, 2012.

[20] X. Wang, M.-H. Meng, and C. Hu, "A localization method using 3-axis magnetoresistive sensors for tracking of capsule endoscope," in *Annual International Conference of the IEEE Engineering in Medicine and Biology Society (EMBS)*, 2006, pp. 2522–2525.

[21] D. Fischer, R. Schreiber, D. Levi, and R. Eliakim, "Capsule endoscopy: the localization system," *Gastrointestinal Endoscopy Clinics of North America*, vol. 14, pp. 25–31, 2004.

[22] X. Xie, G. Li, X. Chen, X. Li, and Z. Wang, "A low-power digital ic design inside the wireless endoscopic capsule," *IEEE Journal of Solid-State Circuits (JSSC)*, vol. 41, no. 11, pp. 2390–2400, 2006.

[23] B. Chi, J. Yao, S. Han, X. Xie, G. Li, and Z. Wang, "Low-power transceiver analog front-end circuits for bidirectional high data rate wireless telemetry in medical endoscopy applications," *IEEE Transactions on Biomedical Engineering (TBE)*, vol. 54, no. 7, pp. 1291–1299, 2007.

[24] X. Chen, X. Zhang, L. Zhang, X. Li, N. Qi, H. Jiang, and Z. Wang, "A wireless capsule endoscope system with low-power controlling and processing asic," *IEEE Transactions on Biomedical Circuits and Systems (TBioCAS)*, vol. 3, no. 1, pp. 11–22, 2009.

Stephen P. Woods received the BEng (Honours) degree in 2008. He is currently employed as Head of Design for Duckworth & Kent Ltd. where he designs surgical instruments for ophthalmology. Additionally, he is working towards the PhD degree at the Centre for Bio-Inspired Technology (Institute of Biomedical Engineering and Department of Electrical and Electronic Engineering) at Imperial College London. His current research interests include microactuators and medical robotic systems.

Timothy G. Constandinou (AM'98-M'01-SM'10) received the B.Eng. degree in Electrical and Electronic Engineering in 2001 and the Ph.D. degree in 2005 both from Imperial College London. He then moved to the Institute of Biomedical Engineering (also at Imperial) where he was appointed to Research Officer in Bionics until joining academic faculty in 2010. He is currently a lecturer within the Department of Electrical & Electronic Engineering at Imperial College London and is also the deputy director of the Centre for Bio-Inspired Technology. His research utilises integrated circuit and microsystem technologies to address challenges in implantable neural prosthetics, brain-machine interfaces, lab-on-chip/wireless capsule endoscope platforms and medical devices in general. He is a Senior Member of the IEEE, a Fellow of the IET, a Chartered Engineer and Member of the IoP and SPIE. He serves on the BioCAS and Sensory Systems technical committees of the IEEE CAS Society, was Technical Program Co-Chair of the 2010 and 2011 IEEE BioCAS Conferences, Technical Program Track Co-Chair (Bioengineering) of the 2012 IEEE ICECS Conference, Technical Program Track Chair (ASICs) of the 2012 BSN Conference and also serves on the IET Prizes and Awards committee.